DEVELOPMENT OF HIGH ACTIVITY, COAL-DERIVED, PROMOTED CATALYTIC SYSTEMS FOR NO$_X$ REDUCTION AT LOW TEMPERATURES

Semiannual Technical Progress Report
April 1, 1999 - September 30, 1999

Principal Investigator: J.M. Calo

Submission Date: July 2000

Project Number: DE-FG26-97FT97267--05

Submitted by:

Brown University
Chemical Engineering Program
Division of Engineering, Box D
Providence, RI 02912

Prepared for:

U.S. DEPARTMENT OF ENERGY
National Energy Technology Laboratory (NETL)

Disclaimer

This report was prepared as an account of work sponsored by an agency of the United States Government. Neither the United States Government nor any agency thereof, nor any of their employees, makes any warranty, express of implied, or assumes any legal liability or responsibility for the accuracy, completeness, or usefulness of any information, apparatus, product, or process disclosed, or represents that its use would not infringe privately owned rights. Reference herein to any specific commercial product, process, or service by trade name, trademark, manufacturer, or otherwise does not necessarily constitute or imply its endorsement, recommendation, or favoring by the United States Government or any agency thereof. The views and opinions of authors expressed herein do not necessarily state or reflect those of the United States Government or any agency thereof.

Patent Information

Yes   No
( )   (X)   Is any patentable subject matter disclosed in the report?
( )   ( )   If so, has an invention disclosure been submitted to DOE Patent Counsel?

If yes, identify disclosure number or DOE Case Number _____

Yes   No
( )   (X)   Are there any patent-related objections to the release of this report? If so, state
               the objections.

TABLE OF CONTENTS

EXECUTIVE SUMMARY

This project is directed at an investigation of catalytic NO_x reduction mechanisms on coal-derived, activated carbon supports at low temperatures. Promoted carbon systems offer some potentially significant advantages for heterogeneous NO_x reduction. These include: low cost; high activity at low temperatures, which minimizes carbon loss; oxygen resistance; and a support material which can be engineered with respect to porosity, transport and catalyst dispersion characteristics.

During the reporting period, the following has been accomplished:

(1) Steady-state reactivity studies in the packed bed reactor were extended to the NO/CO-carbon reaction system as a function of temperature and NO and CO concentrations. It was found that the NO reaction rate increased in the presence of CO, and the apparent activation energy decreased to about 75 ± 8 kJ/mol. In addition, the influence of mass transfer limitations were noted at low NO and CO concentrations.

(2) The packed bed reactor/gas flow system has been applied to performing post-reaction temperature programmed desorption (TPD) studies of intermediate surface complexes following steady-state reaction. It was found that the amount of CO-evolving intermediate surface complexes exceeded that of the N_2-evolving surface complexes, and that both *increased* with reaction temperature. The TPD spectra indicates that both types of complexes desorb late, suggesting that they have high desorption activation energies.

Plans for the next reporting period include extending the temperature programmed desorption studies in the packed bed reactor system to the NO/CO reaction system, including exposure to just CO, as well as NO/CO mixtures.

1.0. PROJECT BACKGROUND AND DESCRIPTION

The reduction of NO over promoted carbon supports offers potentially significant advantages over all currently known methods. Under proper conditions, these systems exhibit high activity with minimal loss of the carbon support. Moreover, they can be effective at very low temperatures, including the range compatible with post-economizer sections of utility boilers (350-450°C). However, the fundamental mechanisms of these catalytic systems are still not sufficiently well known to enable the design of an optimal process which exhibits all the desired characteristics. Here it is proposed to focus on a few selected issues of importance in order to improve the current understanding and develop the means to design such systems. Two approaches in particular appear to be particularly attractive and, consequently, will guide the work proposed here: (1) a "two-stage" process involving the quantitative reduction of NO to N_2O, employing K-promoted or Ni-/Co-La_2O_3-Pt-promoted activated carbon, followed by a second step reducing N_2O to N_2 and O_2; and (2) reduction of NO to N_2 and CO_2 with the same catalytic systems in the presence of the gas phase reducing agents, H_2 and CO.

The current project is directed at an investigation of catalytic NO_x reduction mechanisms on coal-derived, activated carbon supports at low temperatures. Promoted carbon systems offer some potentially significant advantages for heterogeneous NO_x reduction. These include: low cost; high activity at low temperatures, which minimizes carbon loss; oxygen resistance; and a support material which can be engineered with respect to porosity, transport and catalyst dispersion characteristics.

The investigation will concentrate primarily on promising promoter systems like - potassium[1,2,3] and Co/Ni-rare earth oxide-Pt[4]. Such systems have both been shown to be effective for NO reduction at low temperatures (300°C-450°C), with low carbon loss. In particular, the focus is on the investigation of : (1) a novel, "two-stage" process for the complete reduction of NO to N_2 and O_2 *via* N_2O as an intermediate; and (2) the use of H_2 and CO reducing agents in conjunction with the promoted carbon systems.

In order to develop and optimize these approaches, however, the fundamental mechanisms responsible for NO_x reduction in these catalytic systems must be better understood and quantified. This is the principal objective of the current proposal. Temperature programmed reaction (TPR), and post-reaction/chemisorption temperature programmed desorption (TPD)

methods will be used to investigate the mechanisms of NO_x reduction on the selected catalytic systems. These methods will be used to probe the important effects of catalyst formulation and loading, carbon porosity structure, NO concentration, the presence of oxygen, water vapor, and N_2O, and total system pressure on heterogeneous NO_x reduction in these catalytic systems.

The experimental systems used for these studies include a TGA/TPD-MS system and a packed bed reactor/gas flow system to conduct isothermal, steady-state reactivity studies.

2.0. DISCUSSION OF PROGRESS THIS PERIOD

2.1. Experimental

2.1-1. Packed Bed Reactor/Gas Flow System.

A schematic of the packed bed reactor/gas flow system that was developed for performing reactivity measurements is presented in Figure 1. A Kin-Tek gas calibration/mixing system was employed for varying NO and CO concentrations in the feed gas to the packed bed. A NO/NO_x chemiluminescence analyzer (ThermoElectron, Model 12A) and a quadrupole mass spectrometer (Ametek MA 100 MF), pumped by a Varian V250 turbomolecular pump, were used for gas composition analyzes.

The packed bed was contained in a quartz tube placed inside a tube furnace. The tube was 20 cm long, with an internal diameter of 4 mm and a wall thickness of 0.1 mm. Approximately 100 mg of char was placed in the quartz tube and held in place by quartz wool plugs at both ends. It was established that NO did not react on the surface of these plugs by performing blank runs with only the quartz wool plugs in place, and monitoring the compositions of the inlet and exit gases. The furnace was controlled with an Omega temperature controller. A Type K thermocouple was placed about 5 mm from the sample next to the quartz tube. Temperatures from 923-1123K, and NO concentrations covering the range 134 - 475 ppm were used in the NO and NO/CO reactivity studies.

2.1-2. Char Samples.

Phenol formaldehyde resin char, produced from the same batch of synthesized resin was used for the current work. Phenol formaldehyde resins have structural features similar to some of those in coals. The chars produced from these resins behave somewhat like chars produced

3

from low rank coals. However, these chars contain considerably lower levels of catalytic impurities, which can be controlled *via* the preparation technique[5].

The polymer resin was prepared in our laboratory according to the procedure developed by Wójtowicz[6]. Following synthesis, the resin was ground in a mortar and pestle and sieved to mesh sizes +35/-20, corresponding to particle sizes of 420 - 840 μm. The polymer raw resin was pyrolyzed in a tube furnace at 1273 K for 2 hours in flowing ultrahigh purity helium. The resultant particle size range was reduced to 250 - 360 μm as a result of this procedure. Since the surface area of phenol formaldehyde resin char develops rapidly with burn-off at low burn-offs[7,8,9,10], it was decided to activate the char to some extent before the experiments. Consequently, the sample was burned-off in a tube furnace in the presence of air to 5% mass loss. The specific surface area was determined in an Autosorb MP-1 by N_2 adsorption (BET method) to be 270 m^2/g. Initially, the char exhibits a very sharp distribution of micropores with a mean located at 7Å.

2.1-3. Experimental Procedures.

For a typical reactivity run, samples were outgassed for 2 hours at 1223K in flowing helium to remove residual surface complexes. The samples were cooled in the helium flow to 400K and then heated at 20 K/min to the desired reaction temperature. The gas flow was then switched to the reaction mixture. The sample was allowed to react for 1 - 3 hours, depending on the reactant gas mixture and temperature, in order to attain a pseudo-steady-state reaction rate. During reaction, the chemiluminescence analyzer and mass spectrometer were used to periodically take measurements of the gas composition.

The chemiluminescence analyzer was calibrated with a commercially prepared and certified gas mixture of 475 ppm NO in helium, purchased from Med-Tech Gases.

He/NO mixtures were prepared by using a KIN-TEK apparatus capable of mixing gases up to 500 ppm in a carrier gas flow. A total flow rate of 100 sccm was used in the reactions. He/CO mixtures were prepared in a mixing tank according to partial pressure measurements.

Blank runs were performed with just the quartz tube and the quartz wool to ascertain the relative importance of NO reduction on the quartz surfaces of the apparatus. The NO-carbon reaction has been previously shown to be catalyzed by both char and quartz under certain conditions[11]. However, Johnsson *et al.* [12] observed that reaction conditions play a key role in the relative importance of the char-catalyzed reaction in comparison to the quartz-catalyzed reaction.

It should be noted that in these latter experiments the CO concentrations used were between 2500 ppm and 3%, whereas in the current work the CO concentrations were between 50 and 500 ppm. A blank experiment was performed with 475 ppm NO in helium, and another with a NO/CO/He (475 ppm NO/500 ppm CO) mixture. Neither of these runs resulted in any observable reduction of NO, as determined with the chemiluminescence analyzer. It was, therefore, concluded that for the concentrations of gases used in the current study, quartz-catalyzed reduction of NO did not play a significant role.

At the end of the reaction run, the gas flow was switched back to pure helium, and the sample was allowed to quench rapidly by shutting off the furnace power and laterally moving the furnace off the packed bed such that the sample zone was instantaneously exposed to ambient temperature. After cooling to 300K, temperature programmed desorption (TPD) of the surface complexes was performed at 20 K/min in a flow of 20 sccm He to approximately 1273K, while monitoring m/e 14, 28, 29, 30, 44, 45, 46 and 32 with the mass spectrometer.

A few different approaches were examined for the absolute calibration of the raw mass spectrometer data. The one that was ultimately used and appeared to be the most consistent was based on the known stoichiometry for the steady-state NO-carbon reaction. The procedure was as follows. First the cracking ratios for nitrogen (m/e 14 and 28) and carbon dioxide (m/e 28 and 44) were determined with pure calibration gases. These data were used to correct the raw signals to signals for N_2, CO and CO_2. The relative sensitivity factor between CO and CO_2 was determined using a mixture of 46.6% CO and 53.4% CO_2. The nitrogen and oxygen atomic balances were then used to determine the absolute calibrations for the three gases of interest. The nitrogen and oxygen balances are represented as follows:

$$NO(in) - NO(out) = 2N_2(out)$$

$$NO(in) - NO(out) + CO(in) = CO(out) + 2CO_2(out)$$

This procedure was performed for each run, and the resulting calibrations were then applied to the temperature programmed desorption (TPD) data.

2.2. Results

2.2-1. The Steady-State NO/CO-Carbon Reaction.

The steady-state reaction behavior of the NO-carbon reaction was presented and discussed in the previous report. Here we present data on the steady-state behavior of the NO-CO-carbon reaction system.

Due to a limited number of data points, it is not possible to make unequivocal conclusions concerning reaction order in the presence of appreciable CO. In Figures 2 and 3, NO conversion is plotted against the NO feed concentration for various for 500 ppm CO and 50 ppm CO, respectively. The data in Figure 3 exhibit a better correspondence to first order behavior in NO.

Further data analysis was done with the assumption that the reaction is first order with respect to NO and zeroth order with respect to CO.[13] Such an analysis leads to the results presented in Figure 4, which is a summary of the reactivities of the NO-CO reactions over resin char. The first thing that is noted is the relative shallowness of the slope of the line for 130 ppm NO/50 ppm CO. At such low concentrations of both gases, the surface is probably unsaturated with respect to surface complexes, and mass transfer limitations may arise within the porosity. Another point of interest is the curved nature of the data for 475 ppm NO/50 ppm CO at very high temperatures, which may be indicative of the onset of mass transfer limitations. Additionally, the numbers indicate that reaction rates increase two- to three-fold when CO is present in the NO-carbon system.

In summary, based primarily on the 475 ppm NO/500 ppm CO and 130 ppm NO/500 ppm CO runs, it is concluded that the activation energy for the NO-CO reaction for the current range of partial pressures of the gases, is 75 ± 8 kJ/mol. Figure 5 shows the first order rate constants on a carbon mass basis for the NO-resin char reaction in the presence of CO. The rate constants were calculated using a pre-exponential factor of $3.06 \pm 3.18 \times 10^{-6}$ mole NO/g carbon•s•ppm NO. This relatively large error is primarily due to the small sample of gasification temperatures and low concentrations involved.

2.2-1.1. Mass Transfer Limitations in the NO-Carbon Reaction. In the previous report, evidence of mass transfer limitations was noted in the corresponding Arrhenius plots for the NO-carbon reaction for the experimental conditions investigated. For the current data in the presence of significant amounts of CO, the curve corresponding to 475 ppm NO and 50 ppm CO in Figure 4 exhibits the "tell-tale" downward curvature typical of the onset of mass transfer limitations. As in the case without added CO, this appears to occur at higher temperatures. Therefore, it is (once again) hypothesized, that the reaction is probably less than first order with respect to NO in the high temperature regime, since mass transfer limitations appear to worsen as NO concentration decreases. However, even though the reaction order may not be *exactly* unity, it may still be

relatively close to unity since this assumption results in a linear reactivity plot in some instances. However, the unequivocal resolution of this problem must await further investigation.
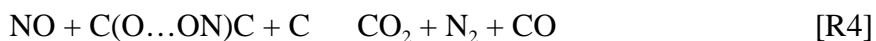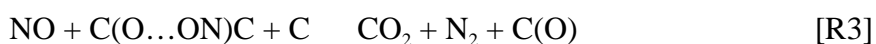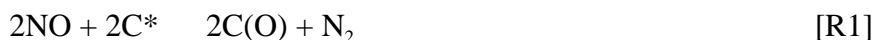
In Figure 4 are presented similar data for the lowest NO concentration investigated (130 ppm NO). In this case, however, there is no evidence of significant curvature indicative of mass transfer limitations. But the curve for the reactivity in 50 ppm CO has a shallower slope in than for the corresponding curve in 500 ppm CO. This could be due to several sources. The experiments performed with 500 ppm CO could still be operating in the chemical reaction rate-controlled regime, while the those performed with the 50 ppm CO could already be operating in the Zone II regime at some temperature below ~900K. Of course, it is also possible that *both* sets of data could already be operating in the Zone II regime.

The difference in slopes could also be an indicator of a non-zeroth order reaction with respect to CO, which is the assumption under which the plots were generated. Results presented by Aarna and Suuberg[14] indicate a zero reaction order with respect to CO, whereas the results of Chan *et al.* [15] indicate zeroth order kinetics for relatively higher values of the CO/NO ratio (~>10) in the feed stream. The resolution of this issue requires more data over a range of temperatures and CO/NO ratios for carbons of varying porosity characteristics.

2.2-2. Temperature Programmed Desorption (TPD) Studies.

2.2-2.1. Background. Temperature programmed desorption (TPD) methods are often used to gather mechanistic clues concerning heterogeneous, gas-solid reaction systems. In the case of the carbon reactivity studies, they have been largely employed to study oxygen surface groups on carbons from CO and CO_2 evolution profiles. TPD spectra, however, are often convoluted by a number of factors such as large numbers of surface species, mass transfer effects, and secondary reactions. These factors can and often influence the CO and CO_2 profiles[16].

In the case of NO-carbon reactions, CO and CO_2 have been observed along with N_2. It is on the basis of the product type and yield that mechanisms have been postulated. Smith *et al.* [17] put forward one of the first mechanisms for NO reduction in 1959:

$$2NO + 2C^* \quad 2C(O) + N_2 \qquad [R1]$$

$$NO + C(O) \quad C(O…ON)C \qquad [R2]$$

$$NO + C(O…ON)C + C \quad CO_2 + N_2 + C(O) \qquad [R3]$$

$$NO + C(O…ON)C + C \quad CO_2 + N_2 + CO \qquad [R4]$$
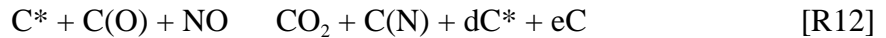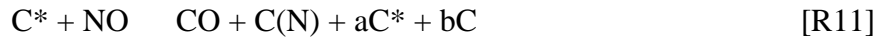
$$2NO + 2CO \quad 2CO_2 + N_2 \qquad [R5]$$

7

[R1] is the dissociative chemisorption of NO on a reactive carbon site, C*. The original presentation of this mechanism contained two reversible steps of the form of [R2], representing the formation of two different types of C(O…ON)C complexes that react with NO according to [R3] and [R4]. [R5] is the NO-CO reaction.

Chan *et al.* [15] proposed a somewhat different mechanism:

$$NO + C^* \quad C(O) + \_N2 \qquad \text{[R6]}$$

$$CO + C(O) \quad CO2 + C^* \qquad \text{[R7]}$$

$$C(O) \quad CO \qquad \text{[R8]}$$

In comparison to the previous mechanism, this one allows for the direct desorption of CO *via* [R8], which is independent of NO. The surface-assisted surface oxide desorption in [R3] is also not included. Chan *et al.* [15] did note the shortcoming of their model in terms of failing to correctly predict an apparent first-order of the reaction rate with respect to NO partial pressure.

Somewhat more recently in our own laboratory, Teng *et al.* [18] proposed the following reaction mechanism for the NO-carbon reaction system:

$$2C + NO \quad C(O) + C(N) \qquad \text{[R9]}$$

$$C + C(O) + NO \quad C(O_2) + C(N) \qquad \text{[R10]}$$

$$C^* + NO \quad CO + C(N) + aC^* + bC \qquad \text{[R11]}$$

$$C^* + C(O) + NO \quad CO_2 + C(N) + dC^* + eC \qquad \text{[R12]}$$

$$C(O) \quad CO + fC^* + gC \qquad \text{[R13]}$$

$$C(O_2) \quad CO_2 + hC^* + iC \qquad \text{[R14]}$$

$$2C(N) \quad N_2 + jC^* + kC \qquad \text{[R15]}$$

where C(O), C(O$_2$) and C(N) are surface complexes, C is a "non-rapid turnover site," and C* is a "rapid turnover site." This mechanism highlights the involvement of different types of carbon active sites in the NO-carbon reduction reaction. Reactions [R9] and [R10] involve dissociative chemisorption of NO on "non-rapid turnover sites," C, thereby indicating that stable surface oxide species are products of these steps. These reactions are probably most important in the low temperature regime. In the high temperature regime, it was proposed that [R11] and [R12] become dominant. The rapid turnover sites in these reactions promptly yield gaseous products promptly. The last three reactions, [R13] – [R15], allow for the formation of surface sites and the relatively slow desorption of gaseous products. These reactions were thought to be governed by a distribution of activation energies. In this model, the stoichiometry of the active sites is

unknown, hence the letter symbols used as the stoichiometric coefficients. It should be noted that this model is thought to apply for relatively pure carbons since no account was taken of catalytic pathways.

Yet another mechanistic step has been proposed more recently by Chambrion *et al.* [19]. These authors postulate that the N_2 formation reaction involves one nitrogen atom from gas phase NO and the other from the surface *via*:

$$C(N) + NO \quad N_2 + C(O) \text{ or } CO \qquad\qquad [R16]$$

While this makes the proposed mechanism even more complex, it appears to have some merit. Functionalities in which surface nitrogen can be found include pyridinic, pyrrolic, quaternary and oxidized nitrogen functionalities[20]. However, it was shown by Chambrion *et al.* [21] that only pyridinic and pyrrolic nitrogen actually participate in reaction [R16]. Quite recently, Chambrion *et al.* also showed *via* physiochemical methods (in an isotopic labeling study) that N2 was mainly formed by the first-order reaction between C(N) and NO in reaction [R16][22].

These mechanisms form the framework against which the TPD results were compared.

2.2-2.2. Experimental   Procedure and General Findings. Pseudo-steady-state NO reduction was achieved on the order of 1 - 3 hours, depending on reaction conditions. The usual procedure for sample preparation in a fixed bed reactor for thermal desorption, is to quench the reaction by switching the gas flow from reactant gases to an inert gas, turn off the furnace, and allow the sample to cool in the inert gas flow. This is followed by thermal desorption at a constant heating in the carrier gas.

It is known, however, that some desorbable species may be lost from the surface in the inert gas flow while the sample remains relatively hot[23]. Consequently, a smaller furnace was constructed to allow for more rapid cooling. In addition, the furnace was designed such that it could be moved off of the packed bed sample when the gas flows were switched, thereby allowing it to cool to room temperature much more rapidly at the rate of ~30K/min.

The major species detected in the gas phase were (in order of decreasing abundance) CO, N_2, and CO_2; N_2O was never detected, although attempts were made to do so.

2.2-2.3. TPD Results Following Reaction With NO. Figures 6-8 present the resultant CO TPD spectra following reaction in 475 ppm NO, 340 ppm NO, and 130 ppm NO, respectively. Some general conclusions are readily apparent. For all three NO concentrations, the total amount of oxygen surface complexes *increases* with reaction temperature. This is similar to what was

found by Suuberg *et al.* in a TGA study[24]. It is also apparent that the total integrated amount of oxygen surface complexes, as well as the desorption rates decrease with NO concentration during reaction. The general decrease in total oxygen surface complexes with decreasing inlet NO concentration during steady-state reaction is presented in Figure 9. In addition, as shown in Figures 6-8, the CO spectra are shifted to high temperatures such that either the peak is not attained by the end of the temperature program, or occurs at higher temperatures than could be attained with the quartz apparatus.

The corresponding nitrogen TPD spectra for the same conditions as in Figures 6-8 are presented in Figures 10-12. As shown, the nitrogen evolution is consistently less than that of CO, but the same general trends with respect to NO concentration and reaction temperature are apparent, as with the CO evolution. The decrease in nitrogen surface complexes with decreasing inlet NO concentration during steady-state reaction is presented in Figure 13.

The presence of nitrogen in the TPD products indicates that there must be some long-lived nitrogen surface complexes. Figures 10-12 demonstrate that nitrogen desorbs later in the desorption process in comparison to CO. Nitrogen can be detected at high temperatures without the presence of NO in the mixture, thereby lending support to mechanistic steps such as those proposed by Teng[18] and Chambrion[19]. These data are consistent with the involvement of C(N) complexes in the formation of N_2 as a product in the NO-carbon reaction.

In Figure 14 is presented the total, post-reaction TPD product yield *vs.* reaction temperature. As shown, total TPD products increase with NO inlet concentration and appear to exhibit a monotonic increase with temperature. This is consistent with similar findings by Suuberg *et al.* [24]. The CO/N_2 ratios are presented in Figure 15, and show that CO is consistently greater in abundance than N_2 for a given data point and that these ratios seem to increase and then decrease as gasification temperature increases.

3.0. PLANS FOR THE NEXT REPORTING PERIOD

During the next reporting period the temperature programmed desorption studies in the packed bed reactor system will be extended to the NO/CO reaction system, including following exposure to just CO, as well NO/CO mixtures.

References

[1] Kapteijn, F., A.J.C. Mierop, G. Abbel, and J.A. Moulijn, Proc. Carbone 84, France, 1984, p.60; JACS Comm.1085 (1984).

[2] Illán-Gómez, M.J., A Linares-Solano, and C. Salinas-Martínez de Lecea, and J.M. Calo, Energy & Fuels, 7, 146, 1993.

[3] Illán-Gómez, M.J., A Linares-Solano, L.R. Radovic, and C. Salinas-Martínez de Lecea, Energy & Fuels, 9, 97, 1995a; 9, 104 (1995b); 10, 158 (1996).

[4] Inui, T.,K. Ueno, M.Funabiki,M.Suehiro,T.Sezume,Y.J.Takegami, Far. Trans. 75,1495 (1979); Inui, T., T. Otowa, and Y, Takegami, Ind. Eng. Chem. Prod. Res. Dev. 21, 56 (1982).

[5] Suuberg, E. M., Wójtowicz, M., Calo, J. M., *Carbon*, **27**, 431, (1989).

[6] Wójtowicz, M., *Ph. D. Thesis*, Division of Engineering, Brown University, (1988).

[7] Su. J. L., and Perlmutter, D. D., *AIChE J.*, **26**, 379 (1985).

[8] Dutta, S., Wen, C. Y., Belt, R. J., *Ind. Eng, Chem. Process Des. Dev.,* **16**, 20, (1977).

[9] Adschiri, T., and Furusawa, T., *Fuel*, **65**, 927, (1986).

[10] Hurt, R. H., Sarofim, A. F., Longwell, J. P., *Fuel*, **70**, 1079, (1991).

[11] Berger, A., and Rotzoll, G., *Fuel*, **74**, 452 (1995).

[12] Johnsson, J. E., and Dam-Johansen, K., *11ᵗʰ International Conference on Fluidized Bed Combustion*, New York, p. 1389 (1991).

[13] Aarna, I., Ph. D. Thesis. Division of Engineering, Brown University, Providence, RI, 1998.

[14] Aarna, I. and Suuberg, E. M., *Fuel*, **76**, 475, (1997).

[15] Chan, L. K., Sarofim, A. F., Beer, J. M., *Combustion & Flame,* **52**, 37, (1983).

[16] Calo, J. M. and Hall, P. J., *Fundamental Issues in Control of Carbon Gasification,* p. 329, Kluwer Academic Publisher, The Netherlands (1991).

[17] Smith, R. N., Swinehart, J. and Lesnini, D., *J. Phys. Chem.,* **63**, 544, (1959).

[18] Teng, H., Suuberg, E. M., and Calo, J. M., *Energy and Fuels*, **6**, 398, (1992).

[19] Chambrion, P., Orikasa, H., Kyotani, T., and Tomita, A., *ACS Div. Fuel Chem. Prepr.,* **41(1)**, 170, (1996).

[20] Suzuki, T., Kyotani, T. and Tomita, A., *Ind. Eng. Chem. Res.*, **33**, 2840, (1994).

[21] Chambrion, P., Suzuki, T., Zhang, Z.-G., Kyotani, T., and Tomita, A., *Energy and Fuels*, **11**, 681, (1997).

[22] Chambrion, P., Kyotani, T., and Tomita, A., *Energy and Fuels,* **12**, 416, (1998).

[23] Lu, W., Ph. D. Dissertation, Division of Engineering, Brown University, 1996.

[24] Suuberg, E. M., Teng, H., Calo, J. M., *23rd Symposium (International) on Combustion*, The Combustion Institute, Pittsburgh, p. 1199, (1991).
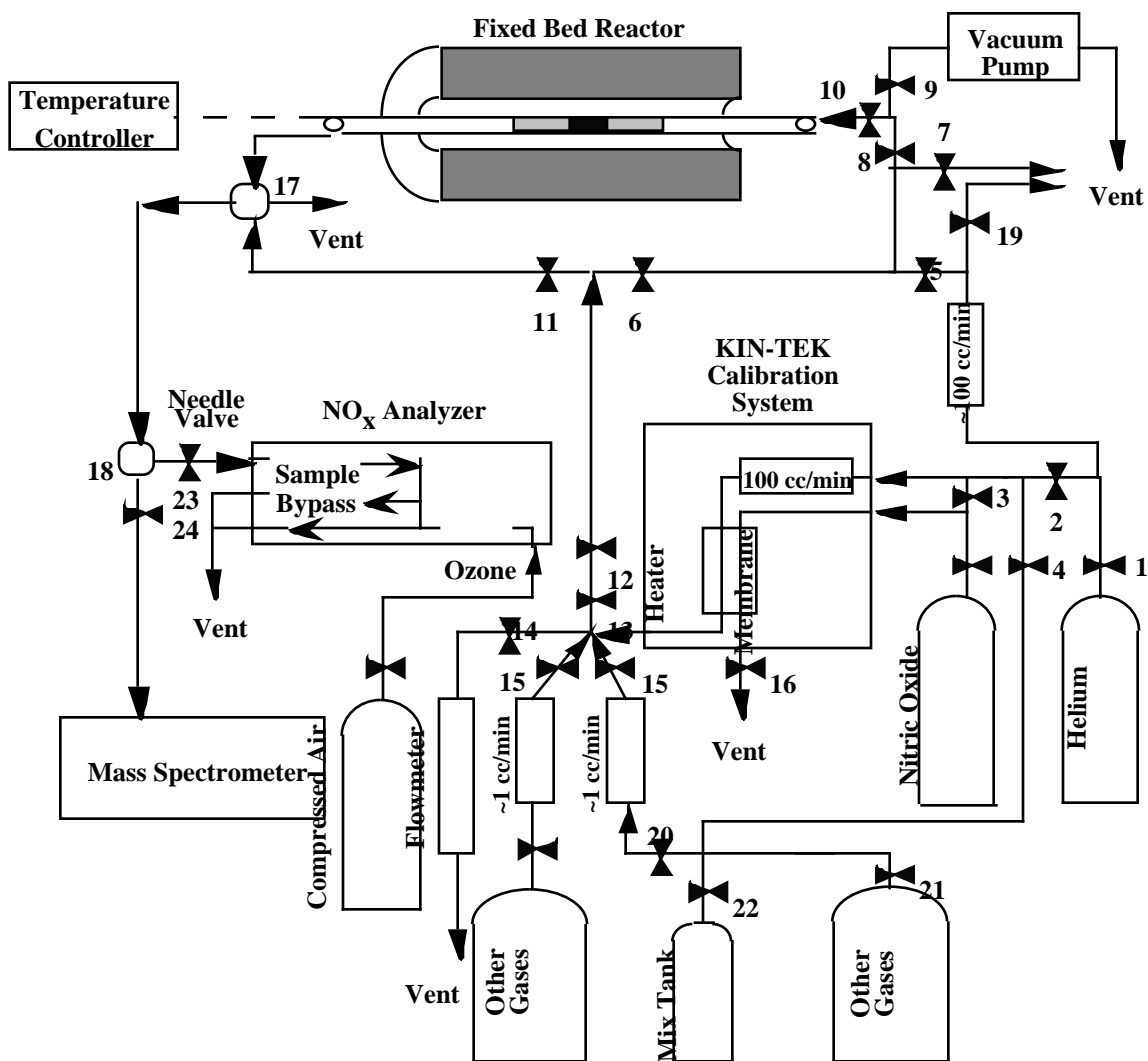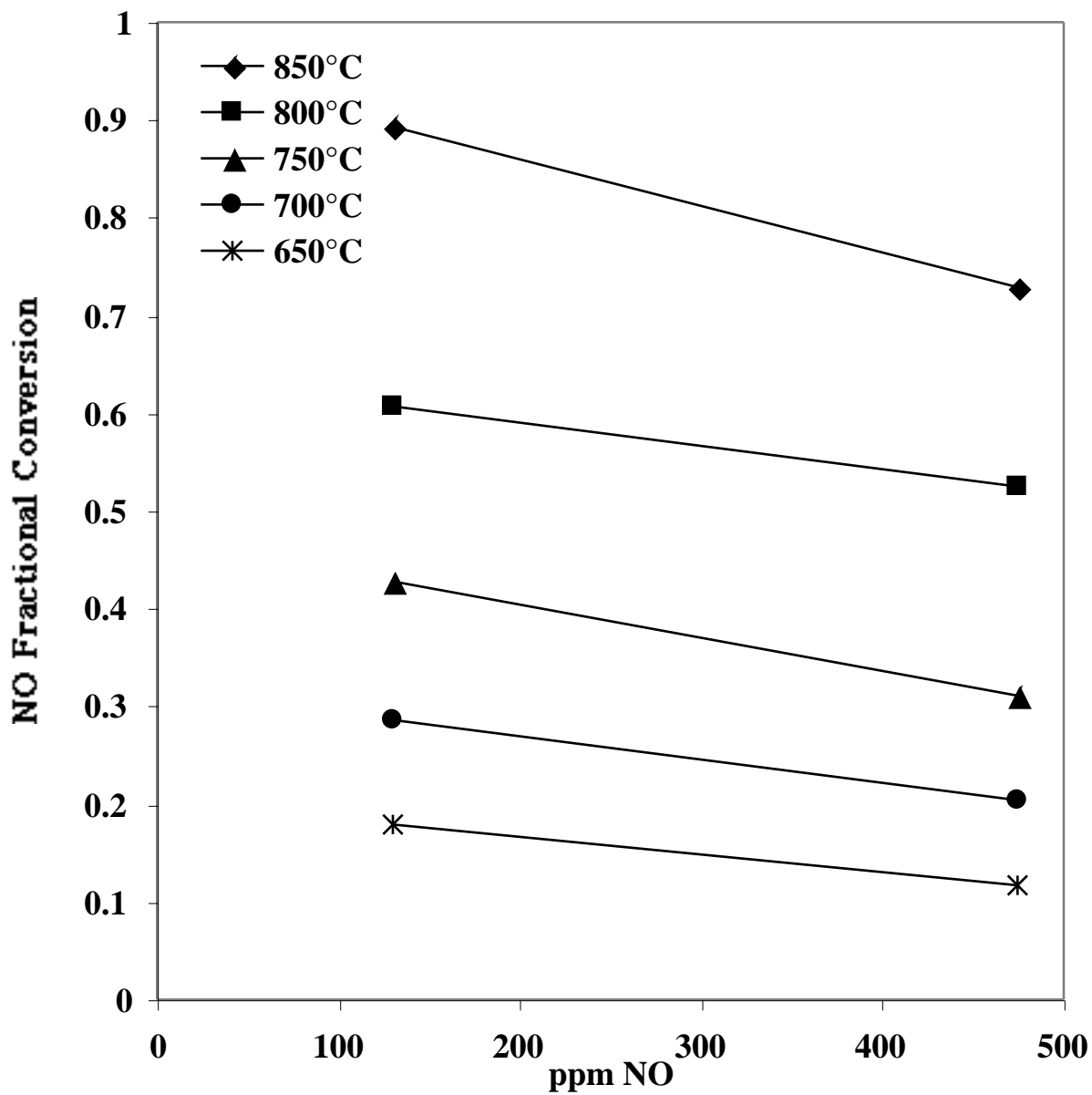
Fixed Bed Reactor

Vacuum Pump

Temperature Controller

10   9

7

8

Vent

17

Vent

19

5

11   6

KIN-TEK Calibration System

~100 cc/min

Needle Valve

NO$_X$ Analyzer

18

Sample Bypass

23

24

Ozone

Vent

12

Heater

100 cc/min

3

2

4   1

13

Membrane

14

15   15

16

Vent

Mass Spectrometer

Flowmeter

~1 cc/min   ~1 cc/min

20

21

22

Vent

Compressed Air

Other Gases

Mix Tank

Other Gases

Nitric Oxide

Helium

Figure 1. Schematic of packed bed reactor system.

Figure 2.   NO conversion in a fixed bed of resin char *vs*. inlet concentration of NO and 500 ppm
CO in a helium carrier gas flow.
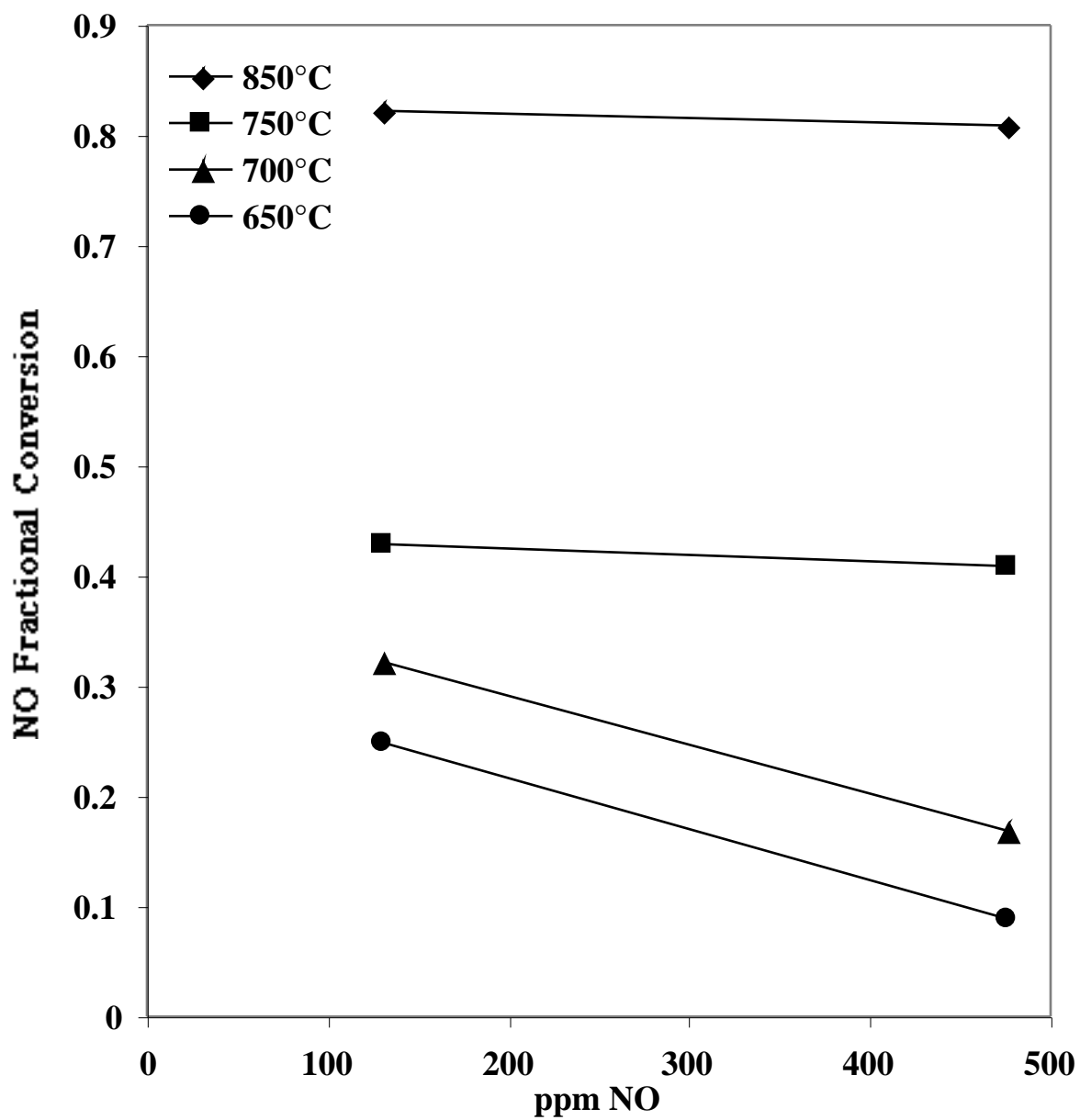
Figure 3.   NO conversion in a fixed bed of resin char *vs*. inlet concentration of NO and 50 ppm
CO in a helium carrier gas flow.
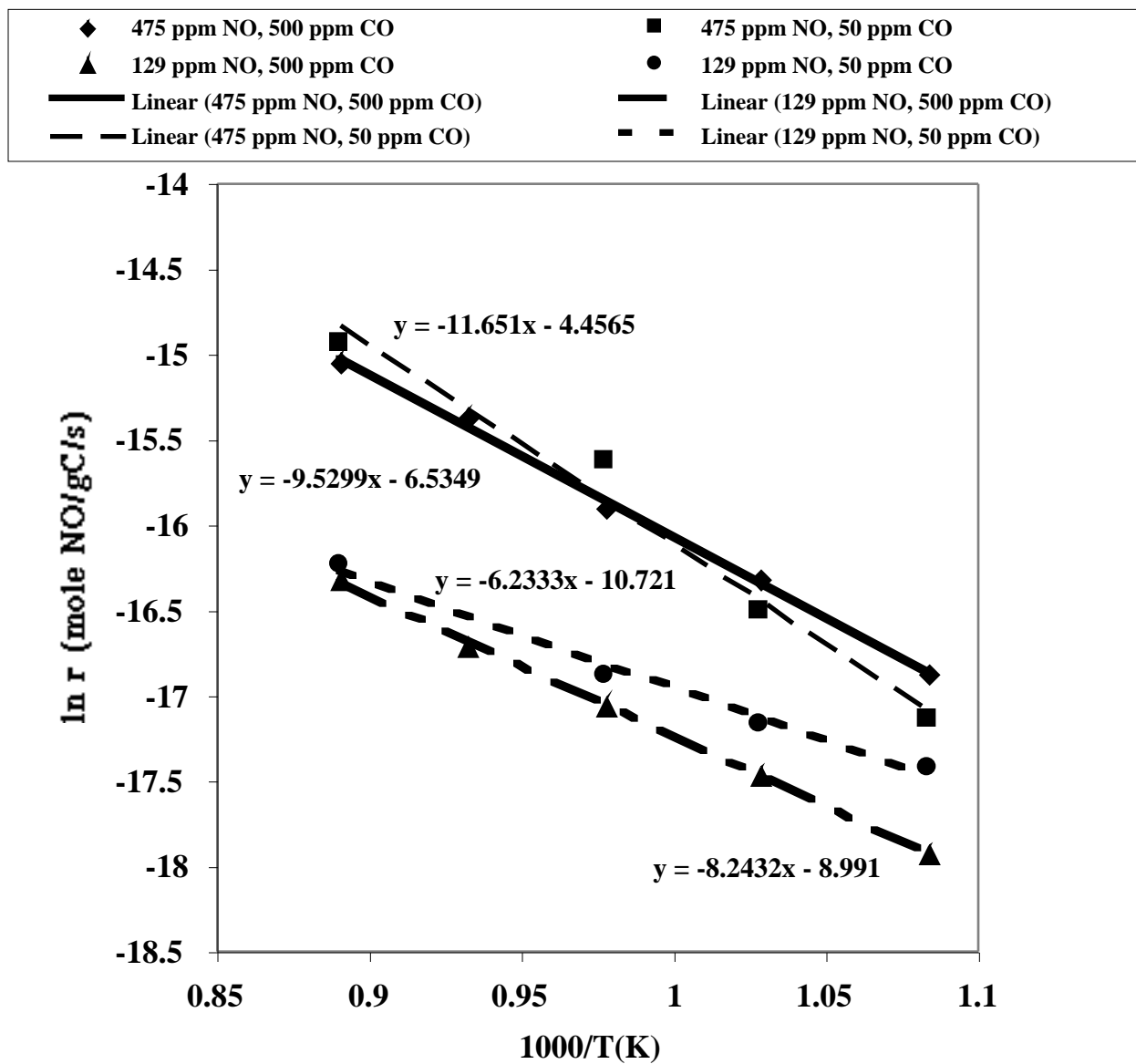
Figure 4. Summary of resin char reactivity in NO/helium mixtures in the presence of CO.
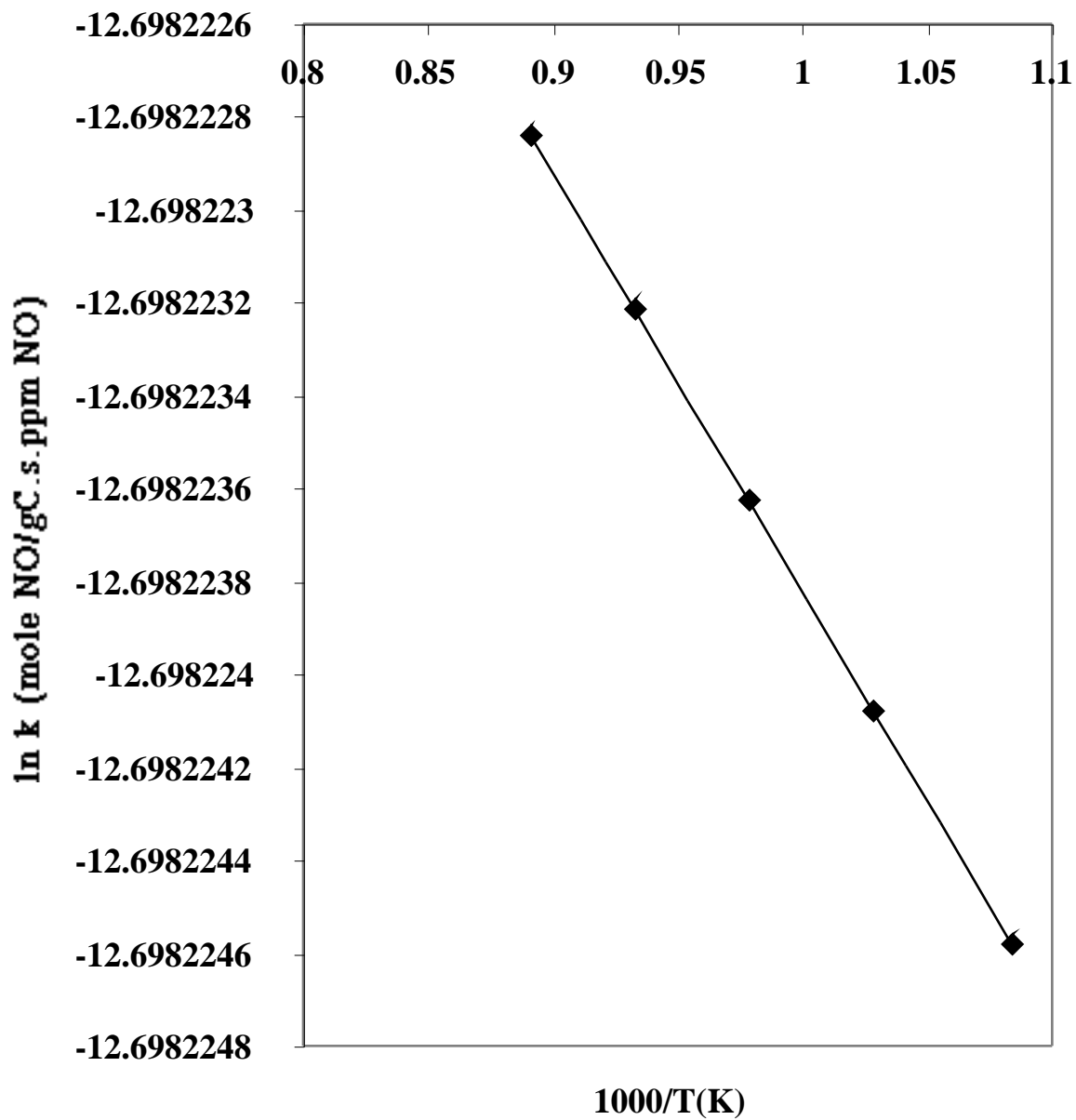
Figure 5.   First order rate constants on a carbon mass basis for the reaction of resin char with NO in the presence of CO.
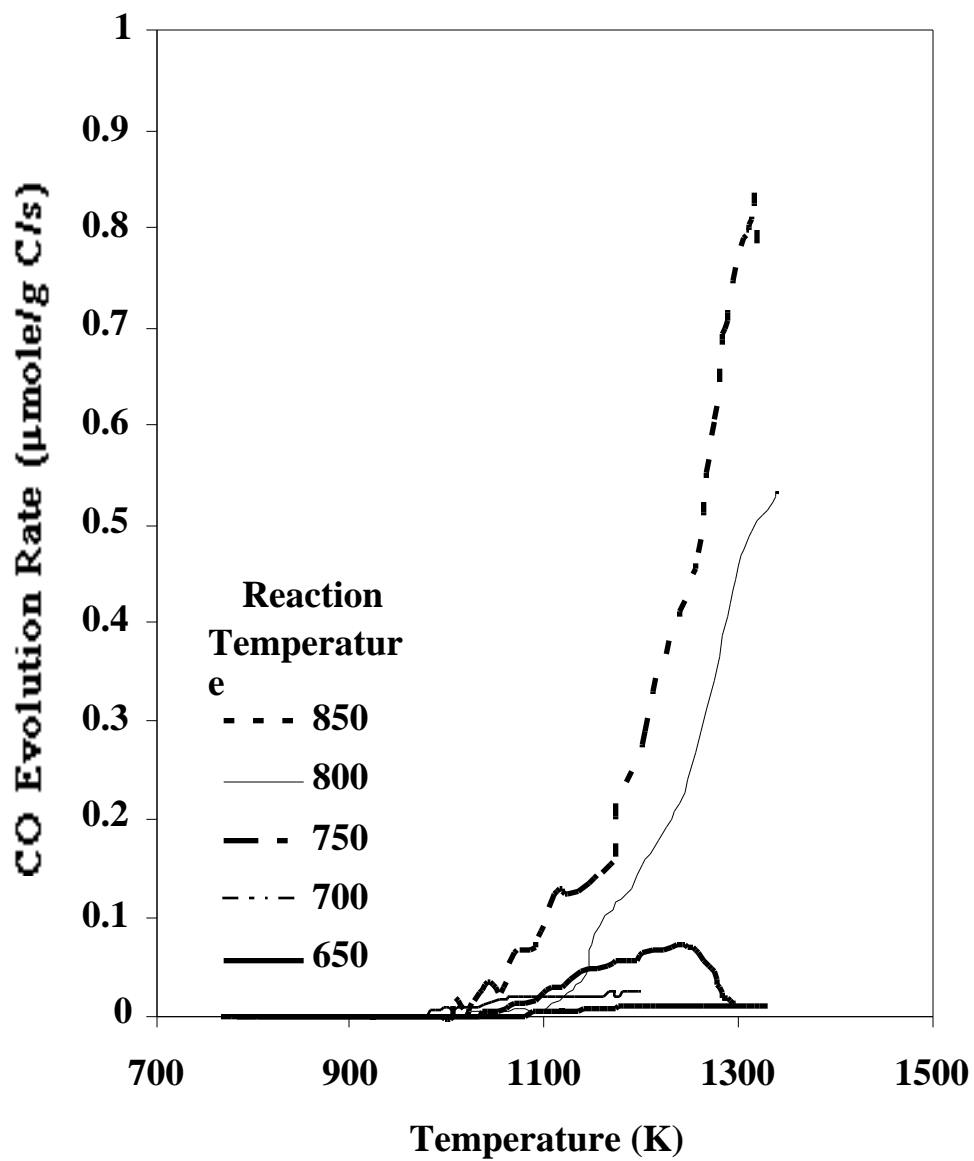
Figure 6. CO TPD spectra following steady-state reaction in 475 ppm NO as a function of reaction temperature.
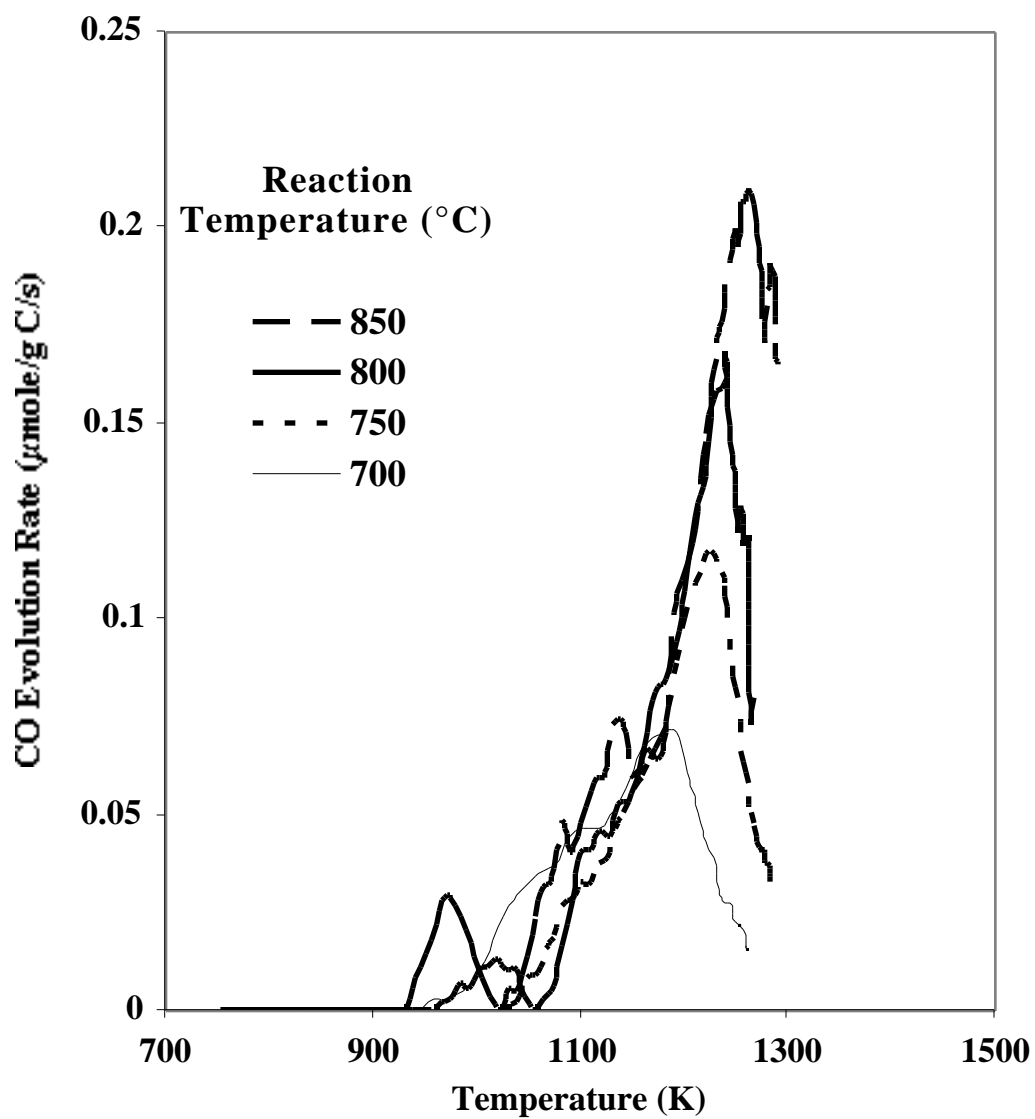
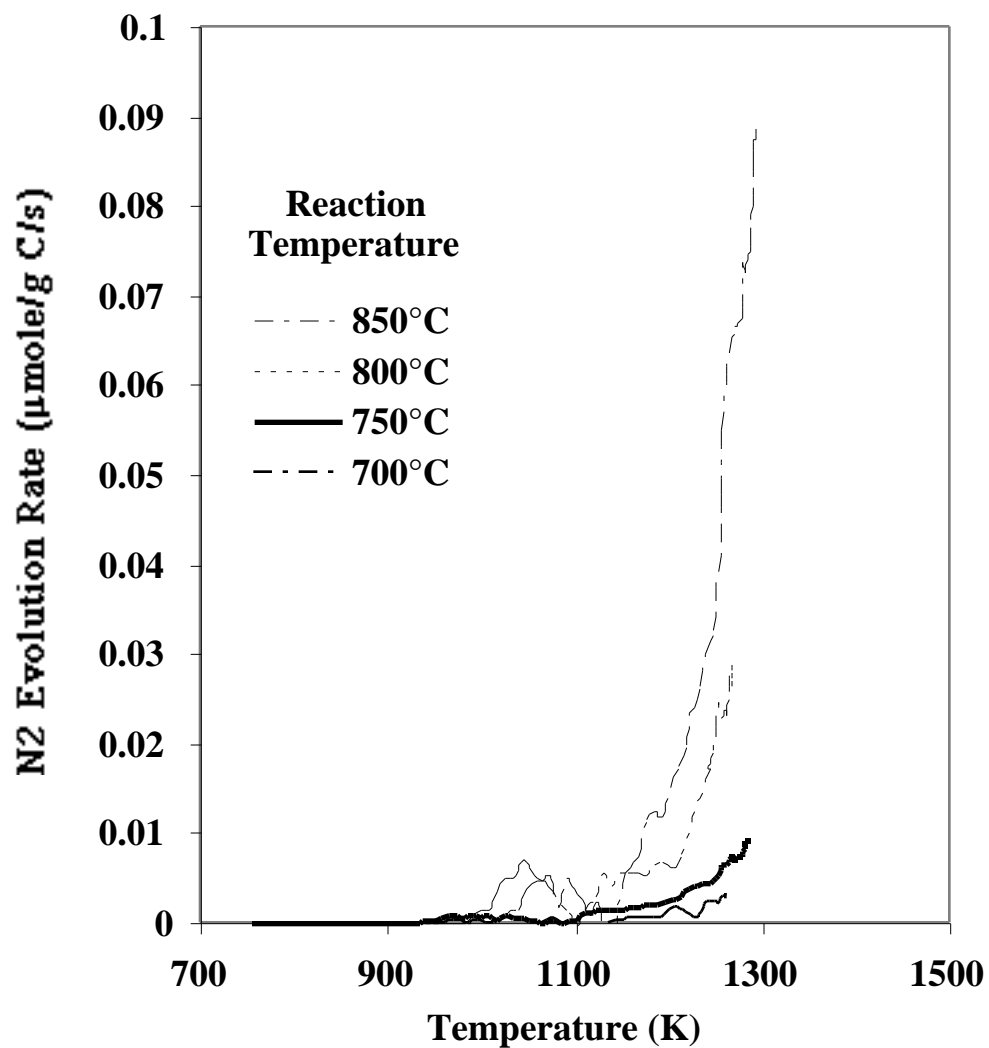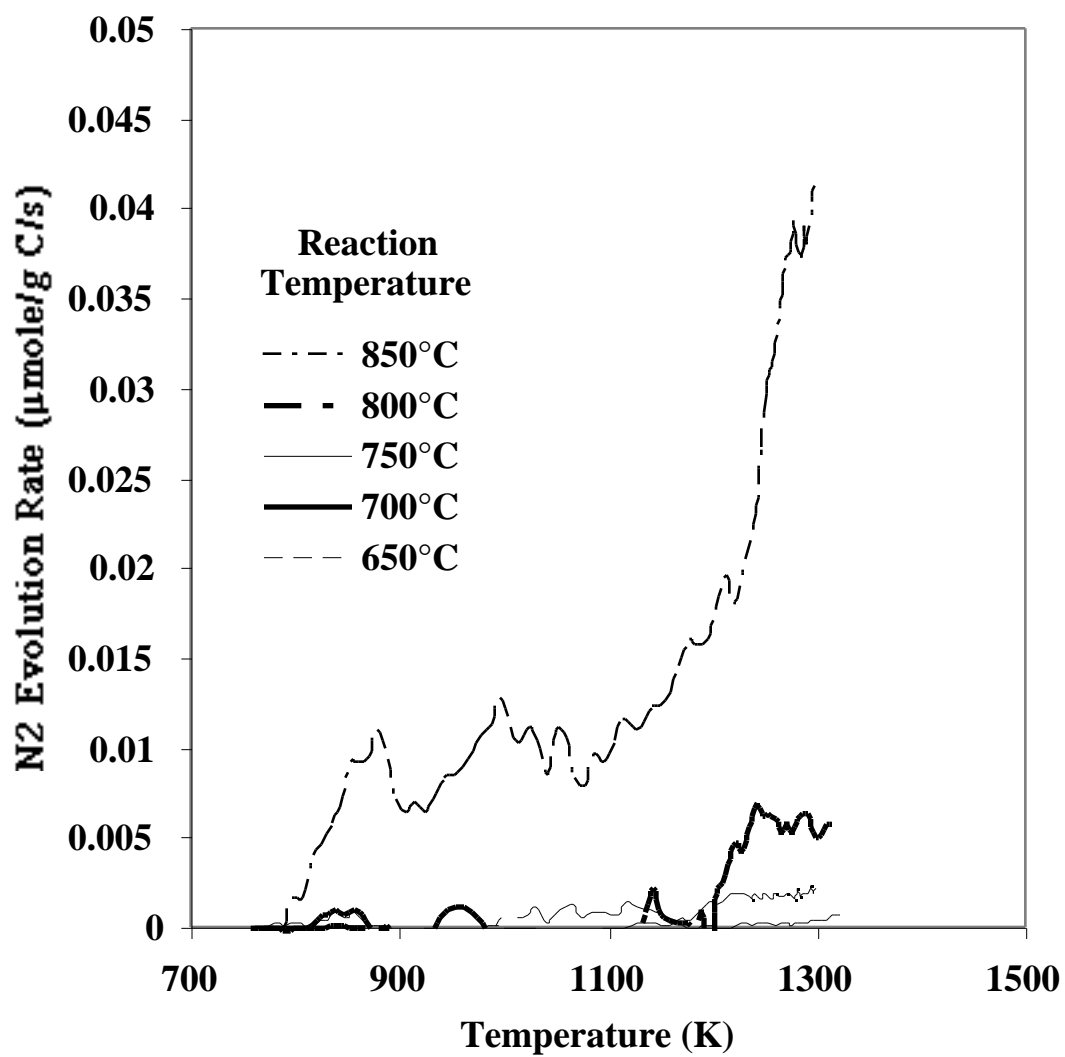Figure 7. CO TPD spectra following steady-state reaction in 340 ppm NO as a function of reaction temperature.
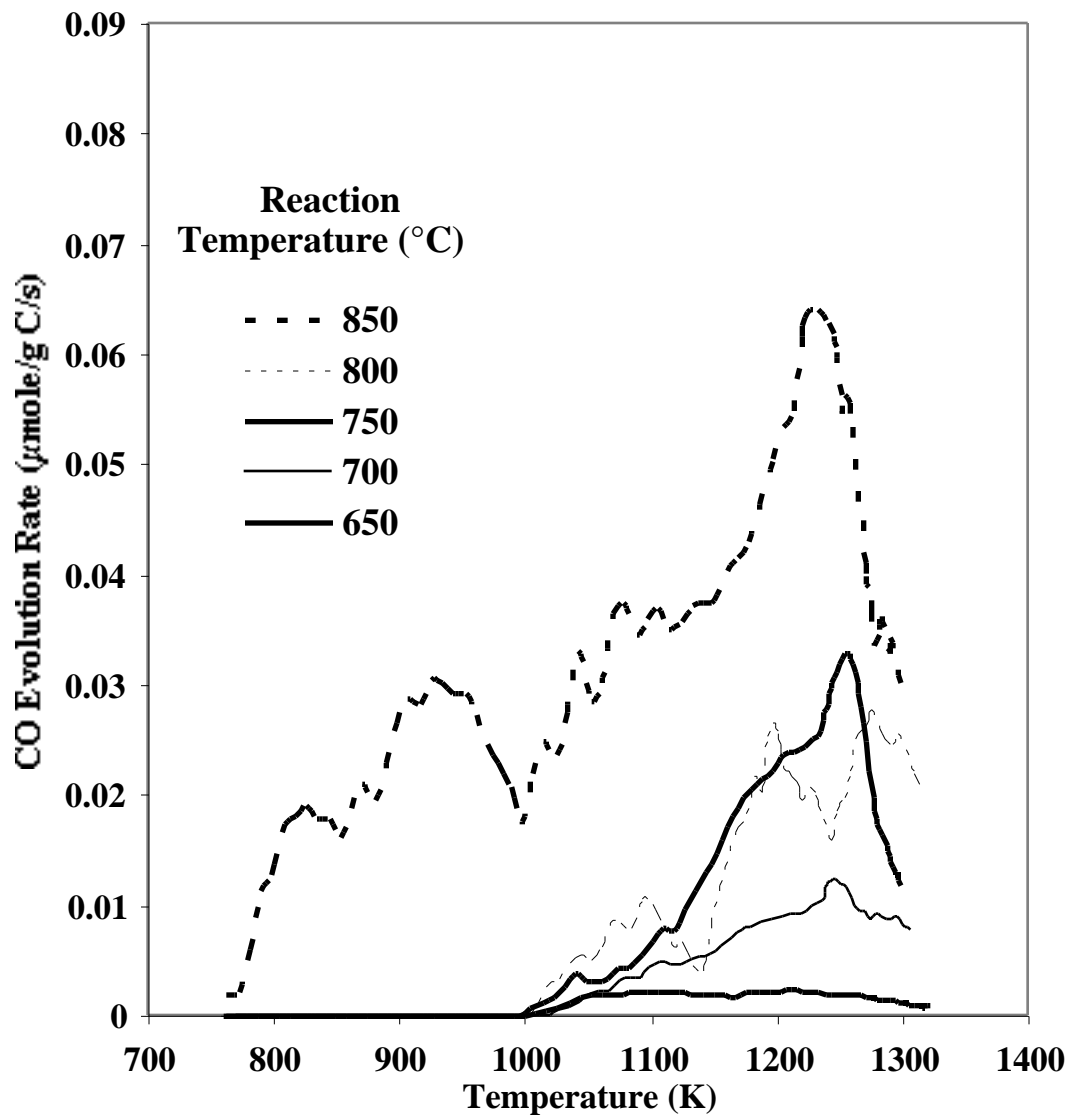
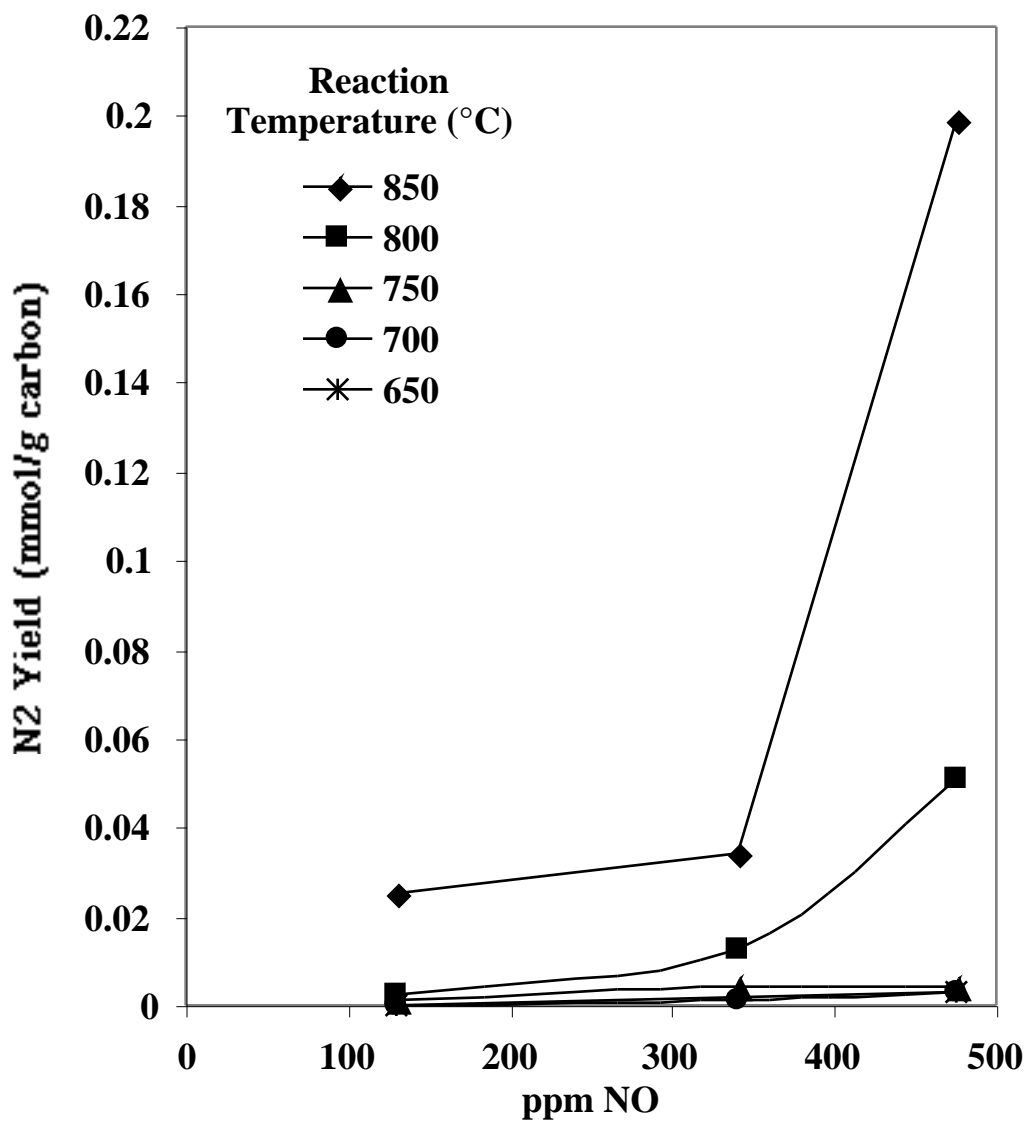Figure 8. CO TPD spectra following steady-state reaction in 130 ppm NO as a function of reaction temperature.
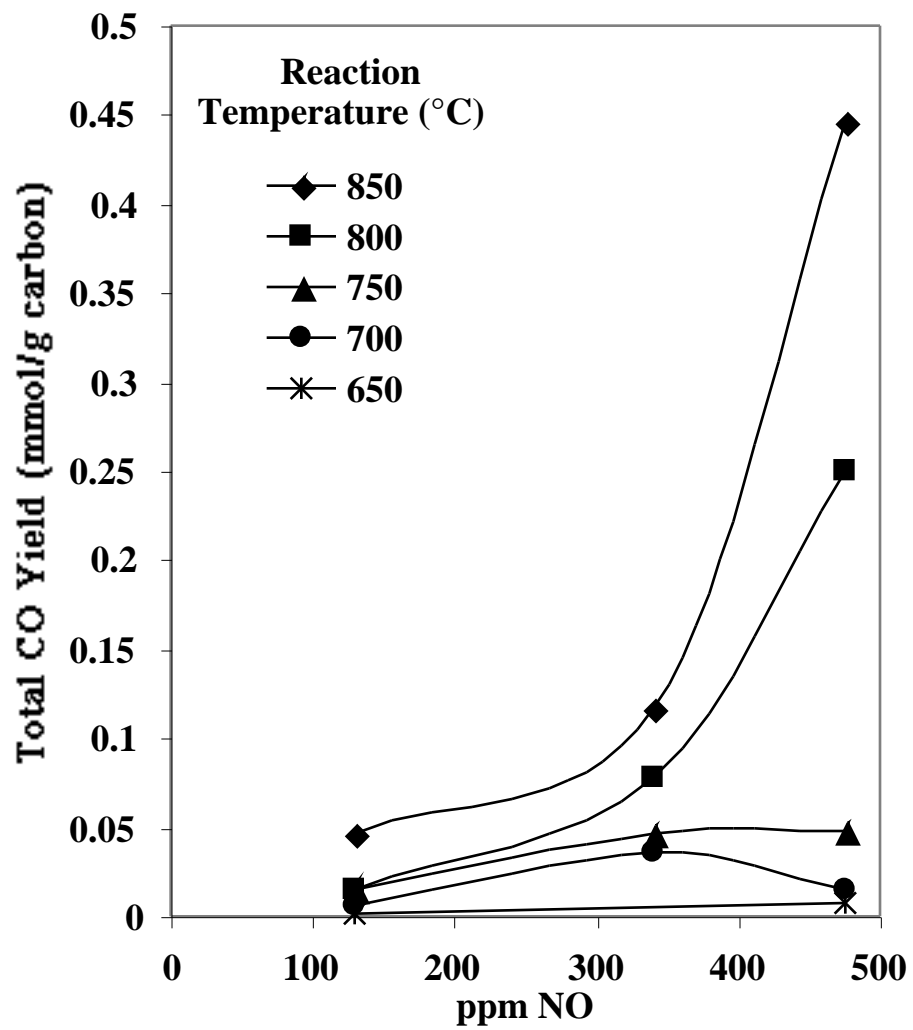
Figure 9. Total CO yields following steady-state reaction as a function of reaction temperature.
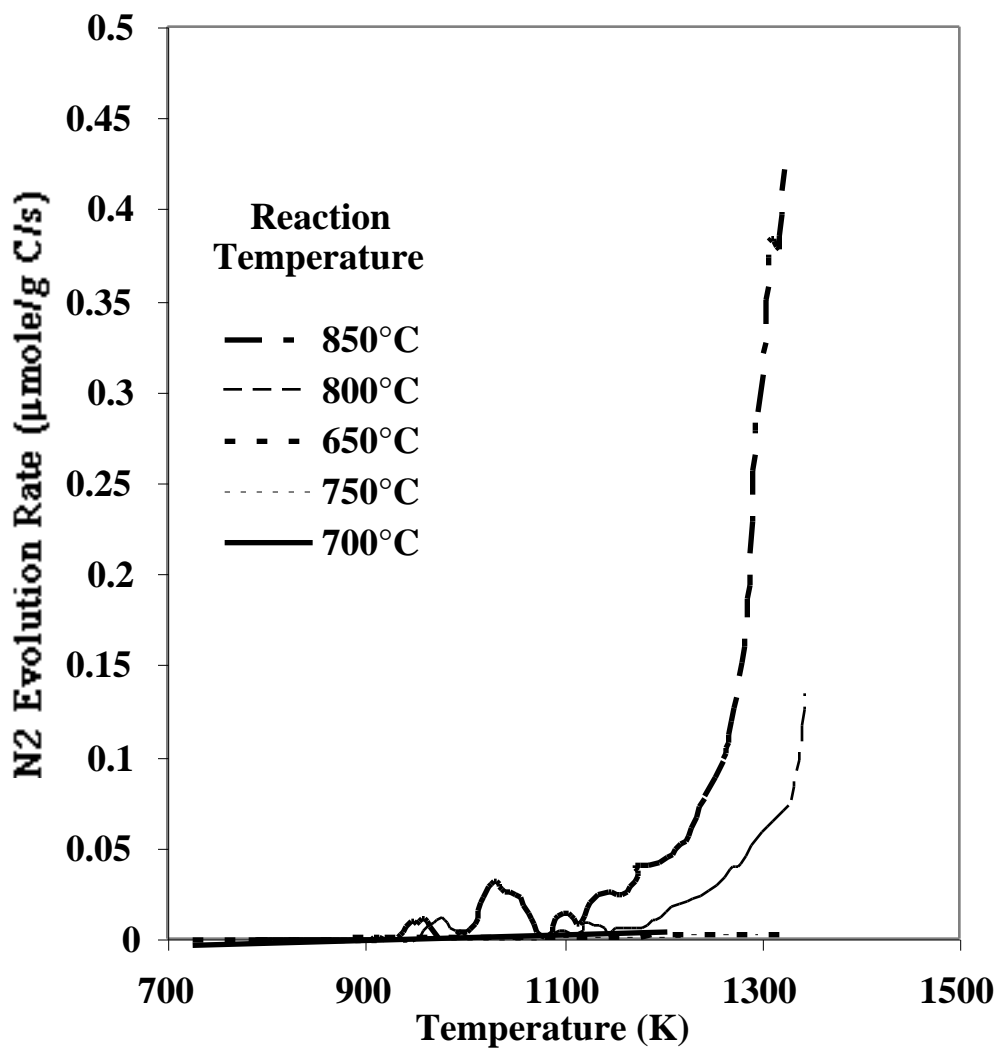
Figure 10. N$_2$ TPD spectra following steady-state reaction in 475 ppm NO as a function of reaction temperature.

Figure 11. N$_2$ TPD spectra following steady-state reaction in 340 ppm NO as a function of reaction temperature.

Figure 12. N_2 TPD spectra following steady-state reaction in 130 ppm NO as a function of reaction temperature.

Figure 13. Total N_2 yields following steady-state reaction as a function of reaction temperature.
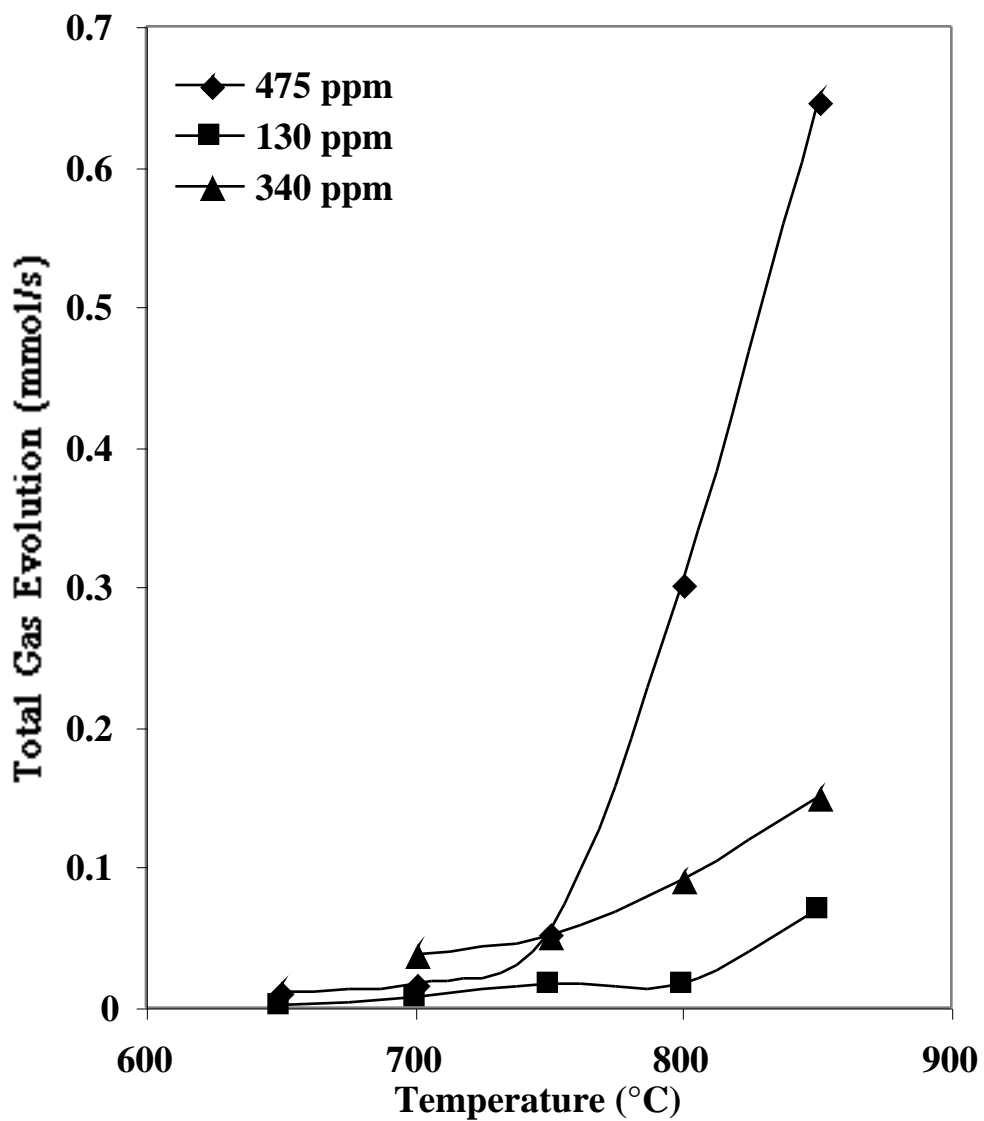
Figure 14. Total gas yields following steady-state reaction as a function of reaction temperature
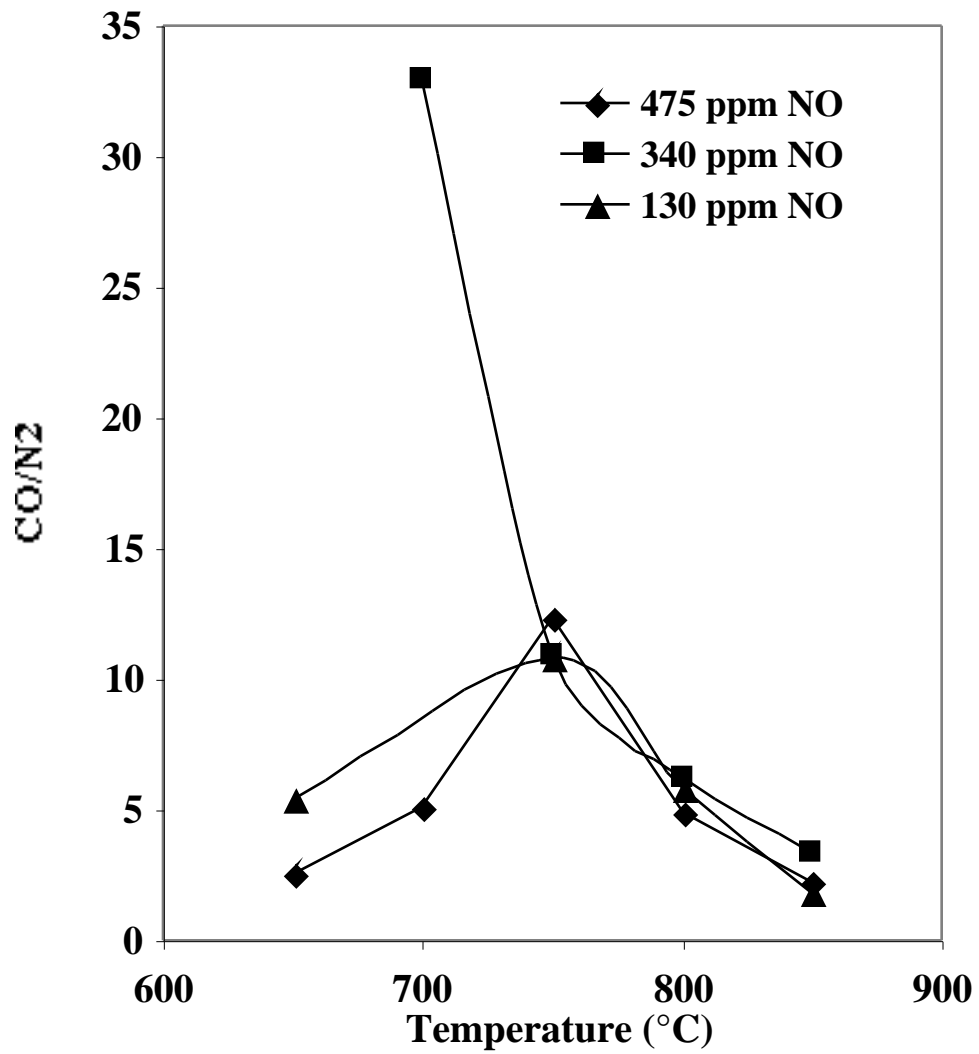for varying NO concentration.

Figure 15. CO/N$_2$ ratios upon TPD following steady-state reaction as a function of reaction temperature for varying NO concentration.